IEEE Access
Multidisciplinary | Rapid Review | Open Access Journal

SPECIAL SECTION ON MULTIPHASE FLOW MEASUREMENT: TECHNIQUES AND APPLICATIONS

Received July 23, 2017, accepted August 3, 2017, date of publication August 15, 2017, date of current version March 15, 2018.

Digital Object Identifier 10.1109/ACCESS.2017.2739918

A Modified Landweber Algorithm for Inversion of Particle Size Distribution Combined With Tikhonov Regularization Theory

MING KONG[1], LIXIA CAO[2], LIANG SHAN[3], AND YAO YANG[1]

[1]College of Metrology and Measurement Engineering, China Jiliang University, Hangzhou 310018, China
[2]Key Laboratory of Energy Thermal Conversion and Control of Ministry of Education, School of Energy and Environment, Southeast University, Nanjing 210096, China
[3]College of Information Engineering, China Jiliang University, Hangzhou 310018, China

Corresponding author: Ming Kong (mkong@cjlu.edu.cn)

This work was supported in part by the National Natural Science Foundation of China under Grant 51476154 and Grant 51404223 and in part by the Natural Science Foundation of Zhejiang Province under Grant LY13E060006 and Grant LQ14E060003.

ABSTRACT Particle size distribution (PSD) measurement based on the static light scattering method has been widely used in the environmental field and combustion diagnostics, such as PM2.5 measurement and combustion process monitoring. The PSD inversion is mathematically related to the Fredholm integral equation of the first kind. Although the Tikhonov regularization algorithm is one of the effective inversion methods to solve the ill-posed linear equation, it still has the disadvantages of excessive smoothness and low accuracy. Thus, a preconditioned Landweber algorithm combined with the Tikhonov regularization theory (the improved algorithm) is proposed in this paper. The Tikhonov regularization theory is used to pretreat the preconditioner B contained in the preconditioned Landweber algorithm. Simulations are conducted to compare the inversion results of the conventional Landweber algorithm, the preconditioned Landweber algorithm, the Tikhonov Chahine algorithm, and the improved algorithm at different signal-to-noise ratios. A CCD-based small-angle forward scattering measurement system is built. A standardized polystyrene microsphere with a diameter of 35.05 μm is used to evaluate the above algorithms. Both numerical and experimental results show that the improved algorithm improves the accuracy of the inversion results and is insensitive to the ring parameter of the detector. The experimental results of the standardized polystyrene microsphere reveal that the relative errors for the median diameter 50 μm are better than 3%. The improved algorithm can provide a highly reliable and stable inversion result.

INDEX TERMS Particle size distribution, light scattering, Landweber algorithm, Tikhonov regularization, CCD.

I. INTRODUCTION

The particle size distribution (PSD) is widely involved in daily life, industrial, and scientific research [1]–[6]. The small-angle forward scattering measurement system has been widely used for the PSD measurement because it is simple, reproducible and easily implemented for online measurement [7], [8]. In the system, the light scattered by the particles is collected by a conventional photodiode detector array consisting of several separate annular rings. However, there is only one fixed ring parameter for each photodiode detector array, making it inconvenient to change the ring parameter. To solve this problem, a CCD sensor is adopted to receive the scattered light instead of the conventional photodiode detector array. Using the CCD sensor, the ring parameter can be set arbitrarily by the image processing technology to extract the scattered light, and the ring structure can be calculated more accurately [9].

The PSD inversion is mathematically the solution of the Fredholm integral equation of the first kind, and is also a typical ill-posed problem, which leads to the instability of its direct solution [10]. The inversion methods are generally classified as the independent mode method and the dependent mode method [11]. In the dependent mode method, the PSD is retrieved by updating distribution parameters of the distribution function. This method requires *a priori* information of the measured particle in advance. In the independent method, the iterative algorithm and the integral transformation are typically used to solve the integral equation.

This work is licensed under a Creative Commons Attribution 3.0 License. For more information, see http://creativecommons.org/licenses/by/3.0/

As a consequence, *a priori* information of the measured particle is not required [12]. Because *a priori* information of the measured particle is usually unknown in the actual measurement, the independent mode method is more promising and more broadly applied compared with the dependent mode method [13].

Presently, the independent mode method has two primary algorithms: the conventional iterative algorithm and the regularization method. The conventional iterative algorithm is usually sensitive to the noise, the ring parameter of the photodiode detector array and the number of iterations because the PSD inversion is a quite ill-posed problem. It is difficult to obtain the stable result. As a result, many scholars have gradually carried out the study of the PSD inversion based on the regularization theory in recent years. Wang presented a linear matrix based on the Tikhonov regularization theory and achieved the stable solution using the relaxation iteration algorithm [14]. Tang used an improved Tikhonov iteration method to retrieve the PSD in the light extinction method [15]. Xu proposed an l_1-norm-based reconstruction algorithm for the PSD inversion in the Fraunhofer diffraction method [16]. In a previous paper by Cao *et al.* [17], the Chahine algorithm in combination with the Tikhonov regularization theory (the Tikhonov Chahine algorithm) was found to be capable of improving the stability and gliding property of inversion results. However, the calculation of the mathematical model based on the Tikhonov regularization theory is time-consuming, and the inversion accuracy is closely related to its regularization parameter and the ring parameter of the photodiode detector array. The Landweber algorithm has the advantage of a simple iterative format and good stability; hence, it is widely used for solving engineering problems [18], [19]. However, the conventional Landweber algorithm is sensitive to its initial value and has a slow convergence rate [20].

To solve the above problems of the conventional Landweber algorithm, a modified algorithm that combines Tikhonov regularization theory with the preconditioned Landweber algorithm (the improved algorithm) is proposed to retrieve the PSD. The Tikhonov regularization algorithm and the preconditioned Landweber algorithm are presented and described. Next, the effectiveness and practicability of the improved algorithm are evaluated by simulations and experiments, respectively. Finally, the inversion results retrieved by the conventional Landweber algorithm, the preconditioned Landweber algorithm, the Tikhonov Chahine algorithm and the improved algorithm are compared using two sets of detector parameters.

II. MEASUREMENT PRINCIPLE OF PARTICLE SIZE DISTRIBUTION

A. MEASUREMENT PRINCIPLE OF THE LIGHT SCATTERING METHOD

In the implementation of the light scattering method, Mie scattering theory has been widely used in the measurement of the PSD. According to the spatial distribution of the scattered light, the PSD can be retrieved [21]. Mie scattering theory is the rigorous solution of the Maxwell equations for uniform spherical particles illuminated by a parallel monochromatic light beam, and is suitable for the PSD inversion of the complex refractive index [22].

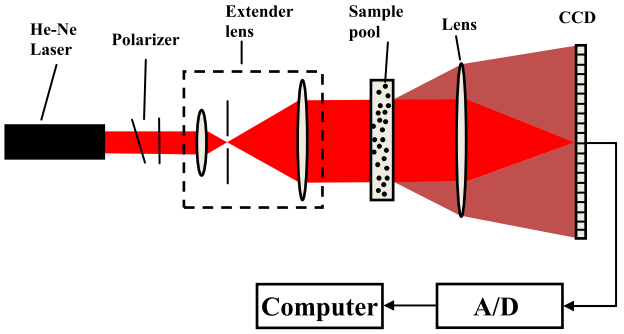

FIGURE 1. Schematic of the small-angle forward scattering system.

The measurement system of the small-angle forward scattering is shown in Fig. 1. A beam from the He-Ne laser (with the incident wavelength of $\lambda = 0.6328\ \mu$m and the operating power of $P = 2.47$ mW) is attenuated to approximately 1mW by the polarizer. Next, the laser passes through an extender lens (with the magnification of $4\times$) so that the laser is collimated, expanded and filtered. The light is scattered by the particles in the sample pool (the cuvette as a sample pool with a cross-sectional area of $s = 10 \times 10$ mm^2) and imaged by the main lens (with the focal length is $f = 25$ mm) on a CCD sensor (1024×1280). The ring parameter (ring radius) of the photodiode detector can be predetermined by the particle size range. The relationship between the particle size range and the ring parameter of the detector is expressed as [23]

$$r_m = \frac{1.357\lambda f}{\pi D_m}, \tag{1}$$

where m is the number of rings, r_m is the m^{th} ring radius, D_m is the particle size corresponding to the m^{th} ring radius, λ is the optical wavelength, and f is the focal length of the lens.

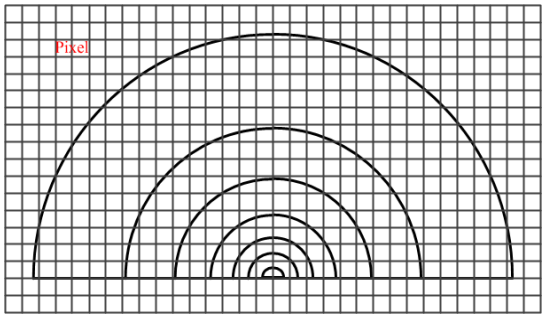

FIGURE 2. Schematic of the photodiode detector array geometry on the CCD sensor.

Finally, the scattered light intensity of each ring (shown in Fig. 2) is calculated by the image processing technique according to the predesigned ring parameter.

For the polydisperse particle system under the condition of the irrelevant single scattering, the relationship between the scattered light intensity on the photodiode detector and the PSD can be expressed as [24]

$$E_i = \sum_i \frac{W_i}{D_i^3} \int_{\theta_{m-1}}^{\theta_m} (i_1 + i_2) \sin\theta d\theta, \tag{2}$$

where m is the number of particle size bins, i_1 and i_2 are the polarized parallel and perpendicular scattered light intensities relative to the scattered plane, respectively, W_i is the weight frequency distribution, D_i is the mean value of each subinterval $[D_m, D_{m-1}]$, and θ_{m-1} and θ_m are the inner and outer radii scattered angle of the m^{th} ring, respectively.

After the discretization of equation (2), it can be expressed in a matrix form as

$$\mathbf{E} = \mathbf{TW}, \tag{3}$$

where $\mathbf{T}$ is the coefficient matrix. According to the Picard criteria [25], the solution of the linear equation (3) can be expressed in a singular system as

$$W = \sum_{i=1}^{\infty} \frac{u_i' E_i v_i}{\beta_i}, \tag{4}$$

where '′' is the transpose, β_i is the singular value of the matrix $\mathbf{T}$, and $\beta_1 \geq \beta_2 \geq \beta_3 \geq \cdots \geq 0$, u_i and v_i are the feature vectors of the matrix $\mathbf{T}$.

The singular value β_i of the coefficient matrix $\mathbf{T}$ tends to be zero because $\mathbf{T}$ is a large and serious ill-conditioned matrix. Thus, the inversion result retrieved by the conventional inversion algorithm deviates from the real value. Therefore, the Tikhonov regularization theory is introduced to improve the linear equation, which can be expressed as [14]

$$(\mathbf{T}'\mathbf{T} + \alpha \mathbf{L}'\mathbf{L})\mathbf{W} = \mathbf{T}'\mathbf{E}, \tag{5}$$

where α is the regularization parameter. According to the Picard criteria, the solution of equation (5) can be expressed in a singular system as [26]

$$W = R_\alpha E = \sum_{i=1}^{\infty} \frac{q_{Tik}(\alpha, \beta_i)}{\beta_i} u_i' E_i v_i \tag{6}$$

$$q_{Tik}(\alpha, \beta_i) = \frac{\beta_i^2}{\alpha + \beta_i^2} \tag{7}$$

The denominator of equation (6) tends to zero at a slower rate than the denominator of equation (4) because of the filter factor $q_{Tik}(\alpha, \beta_i)$. This is useful for the stability of the solution.

B. PRECONDITIONED LANDWEBER ALGORITHM

Lu proposed a preconditioned Landweber algorithm for the computation of ECT imaging reconstruction [27]. The algorithm can be expressed as

$$\begin{cases} \mathbf{W}^{(k+1)} = \mathbf{W}^{(k)} + \omega \mathbf{B}\mathbf{T}'(\mathbf{E} - \mathbf{T}\mathbf{W}^{(k)}) \\ 0 < \omega \leq 1/\|\mathbf{T}\|_2^2 \end{cases} \tag{8}$$

where k is the number of iterations, ω is the relaxation factor and $\mathbf{B}$ is the preconditioner.

Equation (8) can also be expressed in a singular system form as [28]

$$W(k) = \sum_{i=1}^{n} (1 - (1 - \omega\sigma_i\beta_i^2)^k) \frac{u_i' E_i v_i}{\beta_i} \tag{9}$$

$$q_L(k) = (1 - (1 - \omega\sigma_i\beta_i^2)^k), \tag{10}$$

where $q_L(k)$ is the filtering factor related to the number of iterations k, and σ_i is the singular value of the preconditioner $\mathbf{B}$.

The preconditioner $\mathbf{B}$ should be solved before performing the preconditioned Landweber algorithm. The preconditioner $\mathbf{B}$ has the same feature vectors u_i and v_i as those of the matrix $\mathbf{T}$. The preconditioner $\mathbf{B}$ is given by $\mathbf{B} = \sum_{i=1}^{n} u_i \sigma_i v_i'$, The singular value σ_i of the preconditioner $\mathbf{B}$ is given by

$$\sigma_i = \frac{1}{\beta_i^2 + \gamma} \quad or \ \sigma_i = \frac{\beta_i^l}{\beta_i^{(l+1)} + \gamma}, \tag{11}$$

where $l = 1, 2, 3, \ldots$, γ is a constant, $\gamma > 0$.

The calculation of the preconditioner $\mathbf{B}$ is critical to improving the convergence rate and the inversion accuracy of the Landweber algorithm [20]. However, the inversion result retrieved by the above preconditioned Landweber algorithm has the problems of burrs, false peaks and concussion. This leads to the deviation of the retrieved PSD from the real value. Therefore, a modified method for solving the preconditioner $\mathbf{B}$ based on the Tikhonov regularization theory is proposed in this paper. A new singular value β_i is achieved by the singular decomposition of the matrix $(\mathbf{T}'\mathbf{T} + \alpha\mathbf{L}'\mathbf{L})$ of equation (5). The constant γ is determined by

$$\min \left\| \frac{q_L}{\beta_i} - \frac{q_{Tik}}{\beta_i} \right\| = \min \left\| \frac{(1 - (1 - \omega\sigma_i\beta_i^2)^k)}{\beta_i} - \frac{\beta_i}{\alpha + \beta_i^2} \right\| \tag{12}$$

The initial value of the improved Landweber algorithm can be expressed as

$$\mathbf{W}^{(0)} = (\mathbf{T}'\mathbf{T} + \alpha\mathbf{L}'\mathbf{L})^{-1}\mathbf{T}'\mathbf{E} \tag{13}$$

The choice of the regularization parameter is very important for the Tikhonov regularization theory and is also crucial for improving the preconditioned Landweber algorithm. Presently, the Generalized Cross-Validation (GCV) and the L curve method are widely used to calculate the regularization parameter [29]. Both the GCV method and the L curve method have their own advantages and disadvantages [16]. In general, the regularization parameter calculated by the GCV method is greater than that calculated by the L curve. A larger regularization parameter results in an extremely smooth PSD, causing an increase of the PSD width and a loss of the detail of the PSD. This problem usually occurs in the

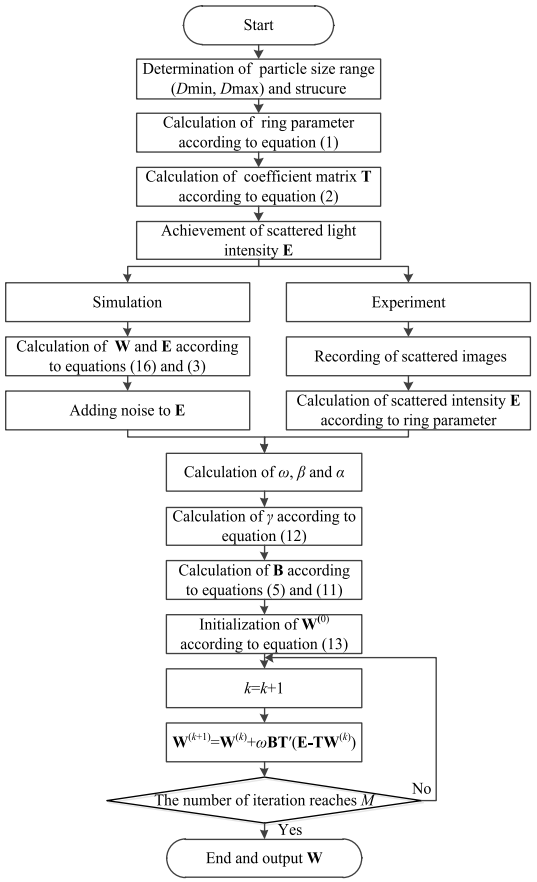

FIGURE 3. Inversion flowchart of the PSD.

inversion of the bimodal PSD. However, a smaller regularization parameter results in a concussive PSD, especially when the scattered light is strongly influenced by the noise. This problem usually occurs in the inversion of the unimodal PSD. As a consequence, the GCV method is used in the case of the unimodal PSD in this paper. The inversion flowchart of the PSD is shown in Fig. 3.

III. SIMULATION AND ANALYSIS

To verify the effectiveness of the improved algorithm, simulations are performed for the homogeneous spheroidal PSD that obeys the unimodal Johnson's SB distribution. Johnson's SB function distribution can be expressed as [30]

$$W(D) = \frac{dt(D_{\max} - D_{\min})}{\sqrt{2\pi}(D - D_{\min})(D_{\max} - D)} \cdot \exp\left\{-\frac{dt^2}{2}\left[\ln\left(\frac{D - D_{\min}}{D_{\max} - D}\right) - \ln\left(\frac{M - D_{\min}}{D_{\max} - M}\right)\right]^2\right\}, \tag{14}$$

where dt is the distribution parameter, M is the mean diameter of the particles, D is the particle diameter, and $D_{\min}$ and $D_{\max}$ are the minimum and maximum values of the particle size range, respectively.

The simulation parameters are shown in Table 1. The particle size ranges from 1μm to 100 μm and is divided into 35 subintervals in the form of the arithmetic sequence $(D_2 - D_1 = D_3 - D_2 = D_4 - D_3 = \cdots = D_i - D_{i-1})$ and 35 subintervals in the form of the geometric sequence $(D_2/D_1 = D_3/D_2 = D_4/D_3 = \cdots = D_i/D_{i-1})$. The ring parameter of the detector is calculated by equation (1). The relative error (Re) is used to characterize the accuracy of the retrieved PSD and can be expressed as [31]

TABLE 1. Parameters of the simulation.

Parameter	Value
Polydispersed particle	(dt, M) =(2.12,44.87)
Monodispersed particle	(dt, M) =(5.5,24.87)
Optical wavelength	λ=0.6328 μm
Fourier lens focal length	f=25 mm
Relative refractive index	m=(1.596-0.1i)/1.33
Particle size range	(1, 100) μm
Signal-to-noise ratio(SNR)	60 dB, 75 dB, 90 dB
Number of test samples in every SNR	20

$$Re = \frac{\sqrt{\sum_i [W_{set}(D_i) - W_{inv}(D_i)]^2}}{\sqrt{\sum_i [W_{set}(D_i)]^2}} \times 100\%, \tag{15}$$

where W_{set} is the theoretical weight frequency distribution, and W_{inv} is the retrieved weight frequency distribution.

The standard deviation (Sd) is used to characterize the stability of the algorithms. The inversion results are shown in Tables 2-3 and Figs. 4-5.

Table 2 shows the inversion results when the particle size interval is divided into 35 subintervals in the form of the arithmetic sequence. The relative errors retrieved by the conventional Landweber algorithm, the preconditioned Landweber algorithm and the Tikhonov Chahine algorithm are found to be more than 20% at various SNRs. However, the relative errors retrieved by the improved algorithm are within 20%. Compared with the above three regularization algorithms, the improved algorithm has higher accuracy. In addition, the standard deviation is acceptable. Fig. 4 shows the comparisons of the unimodal PSD retrieved by the four algorithms when SNR=60dB. The improved algorithm can provide more accurate and reasonable PSDs compared with the other three regularization algorithms. The PSDs retrieved by the conventional Landweber algorithm are quite smooth. The PSDs retrieved by the preconditioned Landweber algorithm have some tiny peaks in the initial position of the PSD. The Tikhonov Chahine algorithm gives the concussive PSDs.

Table 3 shows the inversion results when the particle size interval is divided into 35 subintervals in the form of the geometric sequence. The preconditioned Landweber algorithm is found to have poor inversion accuracy. With the increase of the noise, the improved algorithm and the Tikhonov Chahine algorithm can provide good inversion results. Fig. 5 shows comparisons of the unimodal PSD retrieved by the four algorithms when SNR=60dB. The results of the comparisons indicate that the PSDs achieved by the improved algorithm

TABLE 2. Inversion results when the particle size interval is divided into 35 subintervals in the form of the arithmetic sequence.

Distribution parameters	The number of iterations	*SNR*/dB	Regularization parameter	Conventional Landweber		Preconditioned Landweber		Tikhonov Chahine		Improved algorithm	
				Re/%	*Sd*	*Re*/%	*Sd*	*Re*/%	*Sd*	*Re*/%	*Sd*
dt=2.12, *M*=44.87	10000	60	0.06	21.78	0.96	33.36	0.89	43.57	0.43	5.44	2.26
	10000	75	0.059	21.90	0.19	32.83	0.13	43.46	0.08	2.19	0.58
	10000	90	0.059	21.97	0.04	32.79	0.03	43.45	0.01	2.25	0.09
dt=5.5, *M*=24.87	10000	60	0.12	32.17	0.73	24.29	7.97	42.35	1.07	15.52	2.64
	10000	75	0.12	32.67	0.14	35.26	2.86	43.10	0.12	16.63	0.50
	10000	90	0.11	32.69	0.02	35.12	0.76	43.13	0.03	16.66	0.07

TABLE 3. Inversion results when the particle size interval is divided into 35 subintervals in the form of the geometric sequence.

Distribution parameters	The number of iterations	*SNR*/dB	Regularization parameter	Conventional Landweber		Preconditioned Landweber		Tikhonov Chahine		Improved algorithm	
				Re/%	*SD*	*Re*/%	*SD*	*Re*/%	*SD*	*Re*/%	*SD*
dt=2.12, *M*=44.87	5000	60	0.0043	21.44	1.64	24.94	1.60	10.99	4.69	9.54	1.42
	5000	75	0.0043	20.52	0.36	28.50	0.30	7.60	1.04	2.41	0.51
	5000	90	0.0042	20.42	0.05	24.31	0.88	8.03	0.37	1.61	0.09
dt=5.5, *M*=24.87	5000	60	0.0043	19.52	1.80	27.28	3.96	10.90	3.84	11.50	2.98
	5000	75	0.0042	14.76	0.46	20.82	1.24	10.78	0.85	5.00	0.79
	5000	90	0.0042	14.44	0.11	27.28	3.96	11.59	0.17	4.69	0.16

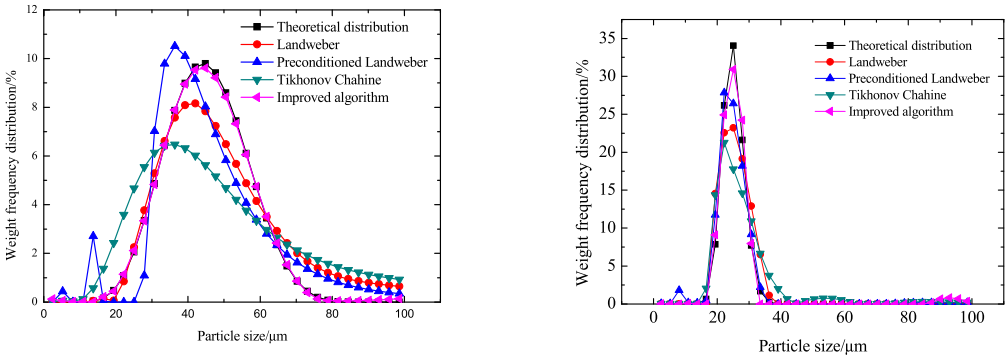

FIGURE 4. Comparisons of the unimodal PSD retrieved by the four algorithms when the particle size interval is divided into 35 subintervals in the form of the arithmetic sequence and *SNR* = 60 dB. (a) Polydispersed particle. (b) Monodispersed particle.

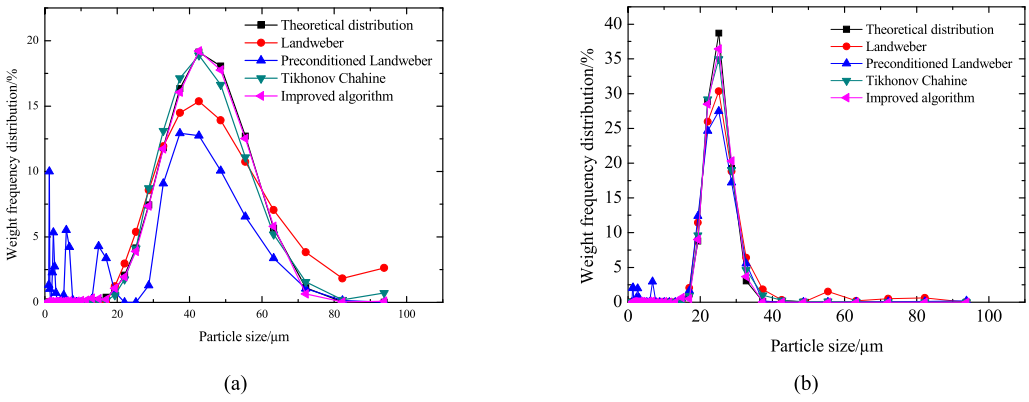

FIGURE 5. Comparisons of the unimodal PSD retrieved by the four algorithms when the particle size interval is divided into 35 subintervals in the form of the geometric sequence and *SNR* = 60 dB. (a) Polydispersed particle. (b) Monodispersed particle.

and the Tikhonov Chahine are almost identical to the theoretical distribution. The width and the peak position of the PSD achieved by the conventional Landweber algorithm deviate from the theoretical distribution. The PSDs retrieved by the preconditioned Landweber algorithm have some tiny peaks in the initial position of the PSD.

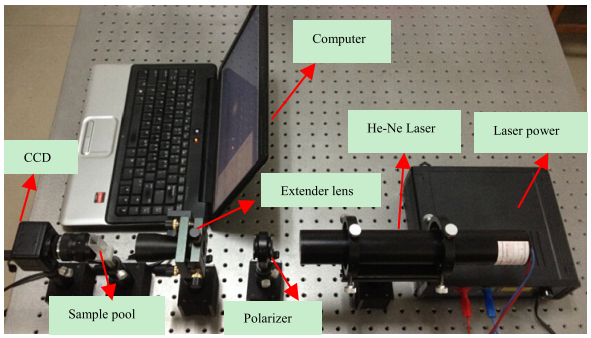

FIGURE 6. Schematic of the experimental system.

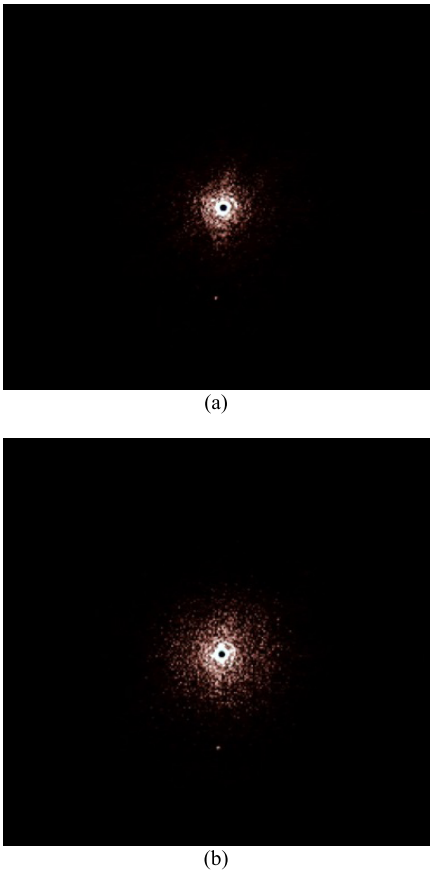

FIGURE 7. Scattered images recorded by the CCD sensor. (a) Scattered image of the sample pool and water. (b) Scattered image of standardized polystyrene microsphere with diameter of 35.05 μm.

From Tables 2, 3 and Figs. 4-5, the improved algorithm is more flexible and can better adapt to the two sets of the detector parameters compared with the other three regularization algorithms.

IV. EXPERIMENTAL RESULTS AND DISCUSSION

Fig. 6 shows a CCD-based small-angle forward scattering measurement system. Its working principle and instrument parameters are presented and described in detail in section II.

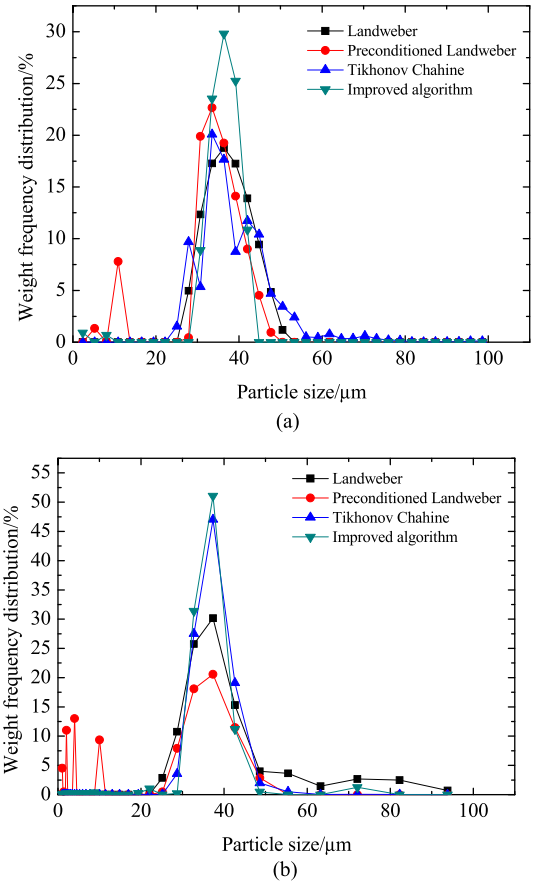

FIGURE 8. Inversion results of the standardized polystyrene microsphere with diameter of 35.05 μm. (a) Inversion results when the particle size interval is divided into 35 subintervals in the form of the arithmetic sequence. (b) Inversion results when the particle size interval is divided into 35 subintervals in the form of the geometric sequence.

A standardized polystyrene microsphere with diameter of 35.05 μm is dispersed in water and then tested. Fig. 7 (a) presents the scattered image of the sample pool without particles (the background image). The scattered image of the particles in the sample pool is shown in Fig. 7 (b). Fig.7 reveals that the level of the scattered light is very high in the focus area. Therefore, the pixels in the center of the CCD sensor will become overexposed, and even overfilled. This overexposure causes a dark spot in the center of the CCD sensor and saturates the pixels in the surrounding area of the dark spot. As a result, in the design of the ring parameter, the inner radius should be designed to be slightly larger than the saturated zone.

According to equation (2), the scattered light distribution E must be achieved before retrieving the PSD. In fact, Fig. 7 (b) contains the background signal and the actual scattered light signal. To obtain the actual scattered signal, the background image shown in Fig. 7 (a) should be deducted from the image shown in Fig. 7 (b). Next, the actual image can be divided into several rings according to the ring parameter and the center coordinate. The average gray value of each ring is calculated and is taken as the scattered light distribution E. Subsequently, the inversion algorithms are performed

TABLE 4. Inversion results of the standardized polystyrene microsphere with diameter of 35.05 μm.

Types of subinterval	The number of iterations	Regularization parameter	Conventional Landweber		Preconditioned Landweber		Tikhonov Chahine		Improved algorithm	
			D_{50}/μm	Re/%	D_{50}/μm	Re/%	D_{50}/μm	Re/%	D_{50}/μm	Re/%
Arithmetic sequence	20000	0.052	35.90	2.43	31.15	11.13	36.17	3.2	35.84	2.25
Geometric sequence	10000	0.0042	34.44	1.74	29.96	14.52	35.26	0.6	34.75	0.86

according to the scattered light distribution. The inversion results of the standardized polystyrene microsphere with diameter of 35.05 μm are shown in Fig. 8 and Table 4. The relative errors for the median diameter 50 μm (D_{50}) are calculated.

It can be seen from Fig. 8 and Table 4 that the conventional Landweber algorithm and the preconditioned Landweber algorithm cannot provide reasonable inversion results. Although the relative errors of the median diameter retrieved by the conventional Landweber are better than 4%, the PSDs are extremely smooth. Some tiny peaks are retrieved by the preconditioned Landweber algorithm. The relative errors retrieved by the Tikhonov Chahine algorithm and the improved algorithm are better than 4%. However, when the particle size interval is divided into 35 subintervals in the form of the arithmetic sequence, there are some false peaks in the middle of the PSD retrieved by the Tikhonov Chahine algorithm. Compared with the other three regularization algorithms, the improved algorithm can be adapted to the above two ring parameters. The problems of burrs, false peaks, concussion, etc. are not presented in the above two ring parameters.

V. CONCLUSIONS

In this paper, a modified preconditioned Landweber algorithm combined with the Tikhonov regularization theory was proposed for the PSD inversion. The preconditioner **B** and the constant γ were recalculated according to a new linear equation based on the Tikhonov regularization theory. In the simulations, the inversion results of the conventional Landweber algorithm, the preconditioned Landweber algorithm, the Tikhonov Chahine algorithm and the improved algorithm were presented and compared at different detector parameters. A standardized polystyrene microsphere with diameter of 35.05 μm was tested experimentally. Simulation and experimental results showed that the improved algorithm can provide a high-precision solution using two sets of the detector parameters. Through comparisons and analysis of the inversion results, the improved algorithm is more reliable and stable at different the detector parameters. The improved algorithm is rapid, simple and reliable.

ACKNOWLEDGMENT

The authors thank State Key Laboratory of Clean Energy Utilization and Key Laboratory of Energy Thermal Conversion and Control of Ministry of Education, School of Energy and Environment, Southeast University, Nanjing, China for supporting the research.

REFERENCES

[1] J. Goo, "Development of the size distribution of smoke particles in a compartment fire," *Fire Safety J.*, vol. 47, no. 1, pp. 46–53, Jan. 2012.
[2] Y. Knop, A. Peled, and R. Cohen, "Influences of limestone particle size distributions and contents on blended cement properties," *Construction Building Mater.*, vol. 71, pp. 26–34, Nov. 2014.
[3] Z. He, H. Qi, Q. Chen, and L. Ruan, "Retrieval of aerosol size distribution using improved quantum-behaved particle swarm optimization on spectral extinction measurements," *Particuology*, vol. 28, no. 5, pp. 6–14, 2016.
[4] C. Levoguer, "Using laser diffraction to measure particle size and distribution," *Metal Powder Rep.*, vol. 68, no. 3, pp. 15–18, 2013.
[5] D. Torre, L. H. Bennett, and Y. Jin, "An effect of particle size on the behavior of ferromagnetic materials," *J. Magn. Magn. Mater.*, vol. 324, no. 14, pp. 2189–2192, 2012.
[6] J. Mao and J. Li, "Dust particle size distribution inversion based on the multi population genetic algorithm," *Terrestrial Atmos. Ocean. Sci.*, vol. 25, no. 6, pp. 791–800, 2014.
[7] X. Shen and J. P. Y. Maa, "A camera and image processing system for floc size distributions of suspended particles," *Marine Geol.*, vol. 376, pp. 132–146, Jun. 2016.
[8] S. Shen, S. Yan, C. Zhou, E. Li, and H. Tong, "Research of laser particle sizer based on scattering theory," *Semicond. Optoelectron.*, vol. 30, no. 5, pp. 1797–1800, 2008.
[9] H. Tan *et al.*, "Particle size measurement based on near field scattering," *J. Beijing Univ. Aeronautics Astron.*, vol. 43, no. 2, pp. 1–8, 2016.
[10] D. Kouzelis, S. M. Candel, E. Esposito, and S. Zikikout, "Particle sizing by laser-light diffraction: Improvements in optics and algorithms," *Particle Particle Syst. Characterization*, vol. 4, nos. 1–4, pp. 151–156, 1987.
[11] F. Xu, X. Cai, K. Ren, and G. Gréhan, "Application of genetic algorithm in particle size analysis by multispectral extinction measurements," *China Particuol.*, vol. 2, no. 6, pp. 235–240, 2004.
[12] L. Wang and X.-G. Sun, "Research on pattern search method for inversion of particle size distribution in spectral extinction technique," *Spectrosc. Spectral Anal.*, vol. 33, no. 3, pp. 618–622, 2013.
[13] L. Wang, X. Sun, and F. Li, "Generalized eikonal approximation for fast retrieval of particle size distribution in spectral extinction technique," *Appl. Opt.*, vol. 51, no. 15, pp. 2997–3005, 2012.
[14] Y. Wang, G. Liang, and Z. Pan, "Inversion of particle size distribution from light-scattering data using a modified regularization algorithm," *Particuology*, vol. 8, no. 4, pp. 365–371, 2010.
[15] H. Tang, "Retrieval of spherical particle size distribution with an improved Tikhonov iteration method," *Thermal Sci.*, vol. 16, no. 5, pp. 1400–1404, 2012.
[16] L. Xu, L. Xin, and Z. Cao, "ℓ_1-norm-based reconstruction algorithm for particle sizing," *IEEE Trans. Instrum. Meas.*, vol. 61, no. 5, pp. 1395–1404, May 2012.
[17] L.-X. Cao, J. Zhao, and M. Kong, "Inversion of particle size distribution based on improved Chahine algorithm," *Infr. Laser Eng.*, vol. 44, no. 9, pp. 2837–2843, 2015.
[18] D. Yang, B. Zhou, C. Xu, and S. Wang, "Dense-phase pneumatic conveying under pressure in horizontal pipeline," *Particuology*, vol. 9, no. 4, pp. 432–440, 2011.
[19] B. S. Kim and K. Y. Kim, "Resistivity imaging of binary mixture using weighted landweber method in electrical impedance tomography," *Flow Meas. Instrum.*, vol. 53, pp. 39–48, Mar. 2017.
[20] M. Piana and M. Bertero, "Projected Landweber method and preconditioning," *Inverse Problems*, vol. 13, no. 2, pp. 441–463, 1997.
[21] R. Xu, "Light scattering: A review of particle characterization applications," *Particuology*, vol. 18, pp. 11–21, Feb. 2015.
[22] G. Gouesbet, "T-matrix formulation and generalized Lorenz–Mie theories in spherical coordinates," *Opt. Commun.*, vol. 283, no. 4, pp. 517–521, 2010.
[23] E. D. Hirleman, V. Oechsle, and N. A. Chigier, "Response characteristics of laser diffraction particle size analyzers—Optical sample volume extent and lens effects," *Opt. Eng.*, vol. 23, no. 5, pp. 610–619, 1984.
[24] J. Vargas-Ubera, J. F. Aguilar, and D. M. Gale, "Reconstruction of particle-size distributions from light-scattering patterns using three inversion methods," *Appl. Opt.*, vol. 46, no. 1, pp. 124–132, 2007.
[25] S. Noschese and L. Reichel, "Some matrix nearness problems suggested by Tikhonov regularization," *Linear Algebra Appl.*, vol. 502, pp. 366–386, Aug. 2016.
[26] W. Cheng, Y. Lu, and Z. Zhang, "Tikhonov regularization-based operational transfer path analysis," *Mech. Syst. Signal Process.*, vol. 75, pp. 494–514, Jun. 2016.

[27] G. Lu, L. Peng, B. Zhang, and Y. Liao, "Preconditioned Landweber iteration algorithm for electrical capacitance tomography," *Flow Meas. Instrum.*, vol. 16, no. 2, pp. 163–167, 2005.
[28] T. S. Pan and A. E. Yagle, "Numerical study of multigrid implementations of some iterative image reconstruction algorithms," *IEEE Trans. Med. Imag.*, vol. 10, no. 4, pp. 572–588, Dec. 1991.
[29] N.-H. Zhu and X.-H. Zhao, "Optimal calculation of Tikhonov regularization parameter based on genetic algorithm," *Eng. Mech.*, vol. 26, no. 5, pp. 25–30, 2009.
[30] H. Qi, B. Zhang, Y. Ren, L. Ruan, and H. Tan, "Retrieval of spherical particle size distribution using ant colony optimization algorithm," *Chin. Opt. Lett.*, vol. 11, no. 11, pp. 105–109, 2013.
[31] L. Xu, T. Wei, J. Zhou, and Z. Cao, "Modified Landweber algorithm for robust particle sizing by using Fraunhofer diffraction," *Appl Opt.*, vol. 53, no. 27, pp. 6185–6193, 2014.

MING KONG received the Ph.D. degree in measurement and control technology and instrumentation from Southeast University, China, in 2006. Since 2012, he has been a Professor with China Jiliang University, China. His main research interests include in multiphase flow instrumentation and computer vision.

LIXIA CAO received the M.Sc. degree from the College of Metrology and Measurement Engineering, China Jiliang University, China, in 2015. She is currently pursuing the Ph.D. degree with the School of Energy and Environment from Southeast University, China. Her main research interests are broadly in multiphase flow instrumentation.

LIANG SHAN received the M.Sc. degree in signal and information processing from Southeast University, China, in 2004. She has been an Associate Professor with China Jiliang University since 2014. Her main research interests are broadly in signal processing.

YAO YANG received the B. Eng. degree in measurement and control technology and instrument from Nanchang University, China, in 2009, and the M.Sc. degree from the College of Metrology and Measurement Engineering from China Jiliang University, China, in 2016. Her main research interests are broadly in multiphase flow instrumentation.